Estuarine, Coastal and Shelf Science 117 (2013) 83–93

Contents lists available at SciVerse ScienceDirect

Estuarine, Coastal and Shelf Science

journal homepage: www.elsevier.com/locate/ecss

Mapping changes in the largest continuous Amazonian mangrove belt using object-based classification of multisensor satellite imagery

Wilson R. Nascimento Jr.[a], Pedro Walfir M. Souza-Filho[a,b,*], Christophe Proisy[c], Richard M. Lucas[d], Ake Rosenqvist[e]

[a] Universidade Federal do Pará, Instituto de Geociências, Cidade Universitária, PO Box 8608, 66075-110 Belém, Pará, Brazil
[b] Vale Institute of Technology Sustainable Development, Rua Boaventura da Silva, 955, 66055-090 Belém, Pará, Brazil
[c] Institut de Recherche pour le Développement (IRD), UMR AMAP, Boulevard de la Lironde, TA A51-PS2, Montpellier Cedex 5 F-34398, France
[d] Aberystwyth University, Institute of Geography and Earth Sciences, Llandinum Building, Aberystwyth, Ceredigion SY23 3AD, UK
[e] Solo Earth Observation (soloEO), TTT Mid-Tower 1708, Kachidoki 6-3-2, Chuo-ku, Tokyo 104-0054, Japan

ARTICLE INFO

Article history:
Received 13 February 2012
Accepted 28 October 2012
Available online 9 November 2012

Keywords:
ALOS PALSAR
GIS
JERS
mangroves
synthetic aperture radar
coastal changes

ABSTRACT

Mapping and monitoring mangrove ecosystems is a crucial objective for tropical countries, particularly where human disturbance occurs and because of uncertainties associated with sea level and climatic fluctuation. In many tropical regions, such efforts have focused largely on the use of optical data despite low capture rates because of persistent cloud cover. Recognizing the ability of Synthetic Aperture Radar (SAR) for providing cloud-free observations, this study investigated the use of JERS-1 SAR and ALOS PALSAR data, acquired in 1996 and 2008 respectively, for mapping the extent of mangroves along the Brazilian coastline, from east of the Amazon River mouth, Pará State, to the Bay of São José in Maranhão. For each year, an object-orientated classification of major land covers (mangrove, secondary vegetation, gallery and swamp forest, open water, intermittent lakes and bare areas) was performed with the resulting maps then compared to quantify change. Comparison with available ground truth data indicated a general accuracy in the 2008 image classification of all land covers of 96% (kappa = 90.6%, tau = 92.6%). Over the 12 year period, the area of mangrove increased by 718.6 km^2 from 6705 m^2 to 7423.60 km^2, with 1931.0 km^2 of expansion and 1213 km^2 of erosion noted; 5493 km^2 remained unchanged in extent. The general accuracy relating to changes in mangroves was 83.3% (Kappa 66.1%; tau 66.7%). The study confirmed that these mangroves constituted the largest continuous belt globally and were experiencing significant change because of the dynamic coastal environment and the influence of sedimentation from the Amazon River along the shoreline. The study recommends continued observations using combinations of SAR and optical data to establish trends in mangrove distributions and implications for provision of ecosystem services (e.g., fish/invertebrate nurseries, carbon storage and coastal protection).

1. Introduction

Mangroves are a globally important coastal forest ecosystem that deliver numerous services for local people, store significant amounts of carbon (Donato et al., 2011), and act as habitat and nursery grounds for marine fauna, many of which are commercially important (Alongi, 2002, 2008; Glaser, 2003) and forest that mitigate coastal erosion (Kathiresan and Rajendran, 2005; UNEP-WCMC, 2006; Souza-Filho et al., 2006). To assess their status, several studies have generated maps of mangroves at regional to global levels (Saenger et al., 1983; FAO, 2005; Spalding et al., 2010; Giri et al., 2011), with these primarily utilizing aerial or optical remote sensing imagery (Green et al., 1998). However, the mapping has been compromised by the lack of consistency in the timing of observations, persistence of cloud cover and smoke haze in many coastal regions, and the complexity of the spectral response of mangroves arising from different species, growth stages, substrate types and tidal conditions (Souza-Filho et al., 2011). For similar reasons, the detection of change has remained a significant challenge. For these reasons, a number of studies have investigated the use of Synthetic Aperture Radar (SAR) for mapping and monitoring mangroves. The RADAM Brazil Project highlighted the potential of this technology for geomorphologic mapping, where GEMS 1000

* Corresponding author. Universidade Federal do Pará, Instituto de Geociências, Cidade Universitária, PO Box 8608, 66075-110 Belém, Pará, Brazil.
E-mail address: walfir@ufpa.br (P.W.M. Souza-Filho).

0272-7714/$ – see front matter © 2012 Elsevier Ltd. All rights reserved.
http://dx.doi.org/10.1016/j.ecss.2012.10.005

radar data were acquired over the Amazon region (Herz, 1991). Other studies (e.g., Proisy et al., 2000; Lucas et al., 2007) have also used SAR data for localized studies of mangroves, with these demonstrating additional potential for retrieving structural attributes and biomass.

For mapping mangroves, a number of techniques have been utilized including visual interpretation of airborne (Hertz, 1991) or satellite sensor data (e.g., Prost, 1997; Rebelo-Mochel, 1997; Souza-Filho and Paradella, 2003, 2005; and Souza-Filho et al., 2006), with most focussing on the use of optical data. Sub-metric and metric optical satellite images provided by recent satellite like Geoeye, Ikonos or Quickbird greatly improve thematic information on forest canopies as highlighted by Wang et al. (2004) and Proisy et al. (2007). But their use for regional or global mapping of coastal environments remains too much expensive and the archive is rather limited. Interestingly, the combination of optical and radar imagery often provides a good visual impression of the extent of mangroves as key elements (e.g., texture, form, size, color and patterning) can be recognized and interpreted for mapping (Souza Filho and Paradella, 2005; Rodrigues and Souza-Filho, 2011). However, the quality of interpretation depends on the experience and knowledge of the analyst (Lu et al., 2004) and the process is time consuming, particularly when mapping mangroves across large areas. Automated procedures (e.g., supervised classifications) provide a more quantitative and reproducible approach and, until recently, have largely been pixel-based. Green et al. (1998) compared different pixel-based approaches for mapping mangroves and conveyed that the main issue was the "granulated effect" observed in the derived maps, which was attributed to random variations in the intrinsic characteristics of the forest canopies and underlying surface (Lobo, 1997). Nevertheless, Souza-Filho (2005) successfully used a visual image interpretation of medium spatial resolution Landsat sensor data to generate the first regional map of mangroves in the Amazon-influenced coast of Brazil. Fromard et al. (2004) used a similar approach to detect major changes in mangroves in French Guiana from series of aerial and Spot images. It is to be noted that the first global map of mangroves computed using the same image analysis protocol was generated only recently i.e. 2011 through a pixel-based classification of approximately 1000 Landsat scenes (Giri et al., 2011).

Object-based approaches are a recent development, with these dividing the digital image homogeneous and spatially contiguous regions (Flanders et al., 2003; Walter, 2004). This reduces 'granularity' and facilitates better mapping and discrimination of classes (Lobo, 1997). These are particularly well suited to mapping mangroves, as these often form discrete units that are largely continuous in cover, relative homogeneous in terms of canopy properties, and often organized in zones that parallel the coastal margins. Object-based approaches also allow data from different sources (e.g., optical or SAR data or digital elevation models) to be integrated and can be used to compensate for gaps in times-series as a consequence of, for example, cloud cover. A limitation, however, is the definition of the Minimum Mapping Unit (MMU; Saura, 2002), which can be too large to allow inclusion of all areas of mangroves (i.e., isolated pixels or groups of pixels representing small areas or margins of mangroves may be omitted; Desclée et al., 2006).

This study aimed to utilize the benefits of both SAR data and object-based approaches for mapping and detecting changes in the extent of mangroves along the Brazilian coastline, with focus on an area southeast of the Amazon mouth, known locally as the Amazon Macrotidal Mangrove Coast (AMCC). For the study, Japanese Earth

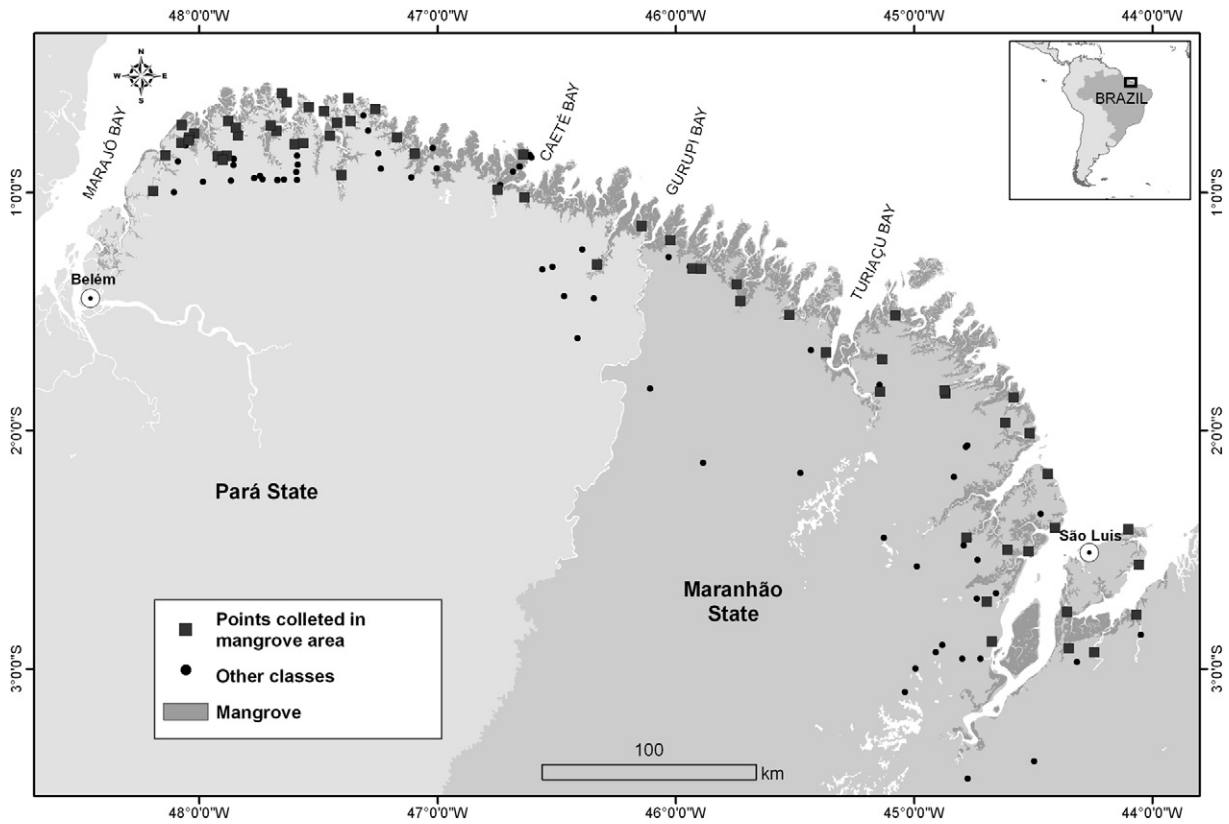

Fig. 1. Location map of the AMM coast between Marajó and São José Bay. See ground control points marked in the study area to validate mangrove classification and change detection.

Resources Satellite (JERS-1) SAR and Advanced Land Observing Satellite (ALOS) Phased Array L-band SAR (PALSAR) data acquired in 1996 and 2008 respectively were used, with these provided through the Japanese Space Exploration Agency (JAXA), a Kyoto and Carbon Initiative. This is an international collaboration led by JAXA that revolves primarily around the ALOS PALSAR (Rosenqvist et al., 2007) and secondly around the Global Rain Forest Mapping (GRFM) project, which provided SAR data from the Japanese Earth Resources Satellite (JERS-1) (Rosenqvist et al., 2000). Both sensors provided cloud-free observations of the AMMC. A limitation of using the SAR data alone was that the boundary between mangroves and adjoining tropical forests was often difficult to establish. Hence, Landsat sensor data acquired over similar time periods were also incorporated to assist with the mapping. The study reports on the accuracy of the maps of mangrove extent in both years and in the detection of change. Recommendations for mapping mangroves using a combination of L-band SAR and optical data are also provided.

2. Study area

The AMMC is located south-east of the Amazon River mouth (Fig. 1) between Marajó Bay (48°W; 0°30′S) and São José Bay (44°15′W; 2° S) and contains the largest and best-preserved mangrove ecosystem in Brazil. Souza-Filho (2005) established that mangroves occupied 7591 km^2 and 56.6% of all mangroves in Brazil, with the mapping undertaken using Landsat-5 Thematic Mapper (TM) images acquired in 2000 and geological and oceanographic data to distinguish five geomorphologic sectors. In this region, the coastline is very jagged with numerous long peninsulas being up to 10 km wide and extending about 30 km out to sea. The coastal currents combined with sediment discharge from the

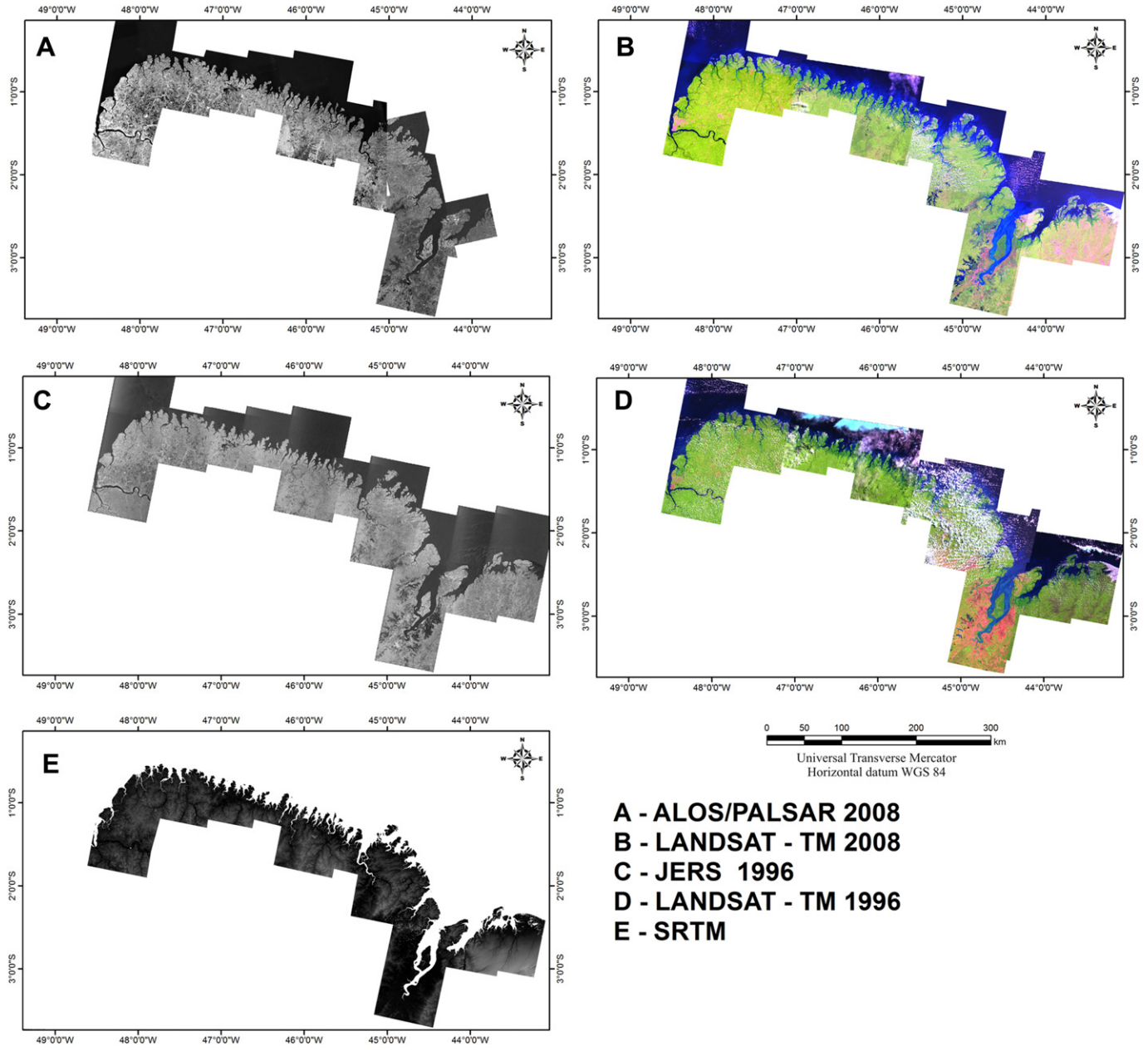

Fig. 2. Mosaic of remotely sensed images.

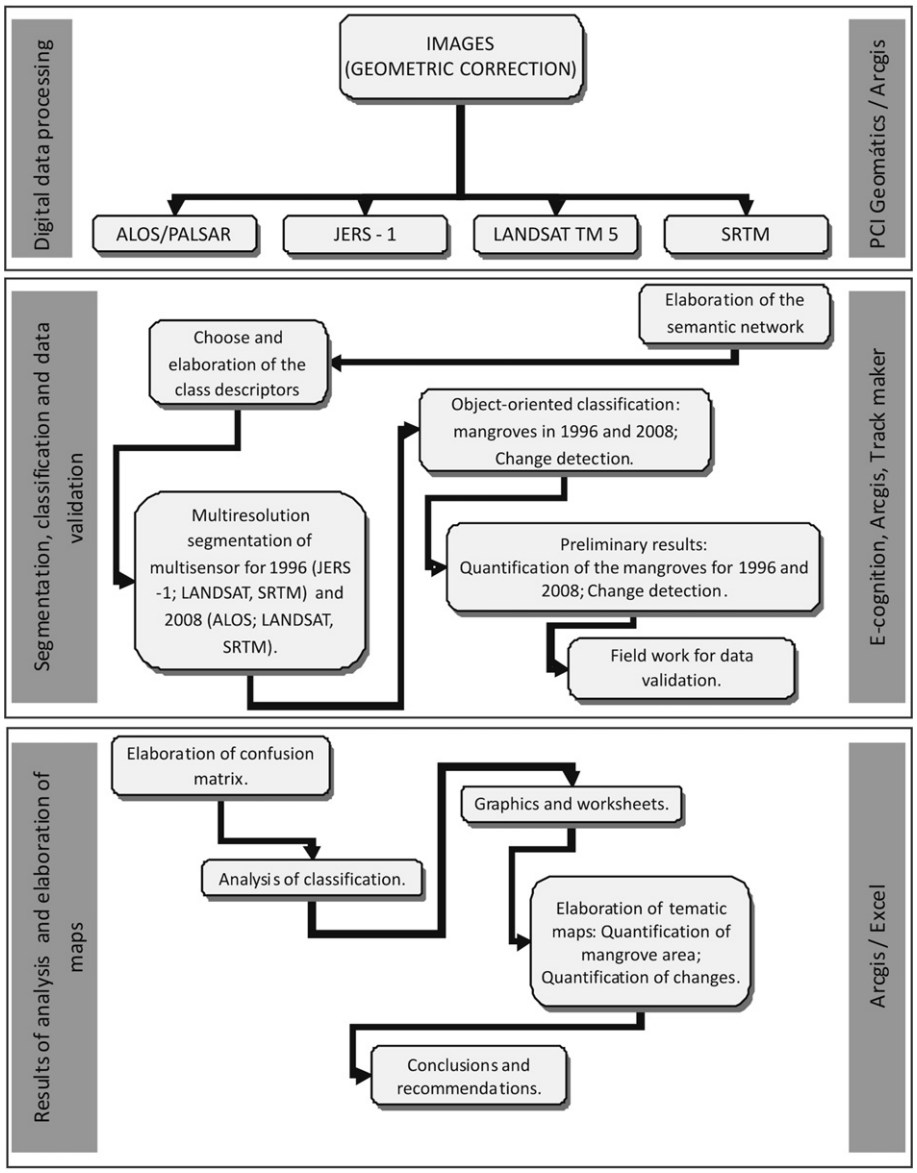

Fig. 3. Flowchart of the processing performed during the research.

Table 1
Characteristics of remotely sensed data.

Satellite/Sensor	Band - wavelength	Polarization	Spatial resolution	Swath width	Incidence angle	Number of images	Acquisition date
ALOS/PALSAR	L-23.5 cm	HH	20 m	70 km	34.3°	Mosaic 18 scenes	From April to September 2008
JERS-1 SAR	L-23.5 cm	HH	18 m	75 km	35°	Mosaic 18 scenes	From November 1995 to March 1996
SRTM	C-5.6 - 7.5 cm	–	90 m	185 km	–	Mosaic	May 2000
Landsat-5 TM	1–0.45–0.52 μm	–	30 m	185 km	98.20°	12	Orbit/Point-Date
	2–0.52–0.60 μm						220/62 - Jun 19, 1995
	3–0.63–0.69 μm						221/61 - Aug 18, 1997
	4–0.76–0.90 μm						221/62 - Oct 16, 1995
	5–1.55–1.75 μm						222/61 - May 13, 1994
	6–10.4–12.5 μm						223/60 - Jun 21, 1994
	7–2.08–2.35 μm						223/61 - Aug 13, 1996
							220/62 - Sep 10, 2008
							221/61 - Jul 29, 2007
							221/62 - Jun 24, 2006
							222/61 - Jun 20, 2008
							223/60 Jul 13, 2008
							223/61 Jul 13, 2008

Amazon River leads to mangroves being highly dynamic in terms of their colonization and loss. The region is also subject to a semi-diurnal macro-tidal regime with variations of around 4 m in Marajó Bay and 7.5 m in São José Bay (DHN, 2010). The climate is governed by seasonal changes in the position of the Inter-Tropical Convergence Zone (ITCZ), which controls precipitation along the Brazilian Equatorial coast and varies from a latitudinal position of around 14° N in August and September and 2° S in March and April. Mean annual rainfall along the studied coast increases westward, from 2250 mm to 2950 mm, with 75% of annual precipitation falling between January and April. In the dry season (September to November), the mean precipitation is close to zero (Moraes et al., 2005). The highest discharges from the rivers occur in April and have been estimated as being 2478, 1393 and 257 $m^3 s^{-1}$ for the Gurupi, Turiaçu and Caeté Rivers respectively (Souza-Filho et al., 2009).

Mangroves in the region are dominated by *Rhizophora mangle*, *racemosa* and *harrisonii* and *Avicennia germinans and schaueriana* species (Menezes et al., 2008). *Laguncularia racemosa* is also observed but as a subdominant species. These mangroves provide a subsistence livelihood for local households of lower income groups with some commercial extraction. Key products include the mangrove crab (*Ucides cordatus*) and mangrove wood and bark (Diele et al., 2010).

3. Materials and methods

The following sections provide an overview of the remote sensing data used for mapping and detecting changes in mangroves between 1996 and 2008. Pre-processing involved calibration and orthorectification of the available imagery, segmentation of the combined dataset and classification using a rule-based approach within eCognition software, with the classification validated primarily using field data. The baseline datasets for the two years were then compared to map areas of change. An overview of the processing is given in Fig. 2.

3.1. Remote sensing datasets and digital image processing

The main steps of the digital image processing and analysis are presented in the flow chart in Fig. 3 and described below. Initially, 2008 ALOS PALSAR, 1996 JERS SAR, 2008 and 1996 Landsat TM images were orthorectified prior to segmentation and classification. The resulting maps of extent and change were then validated

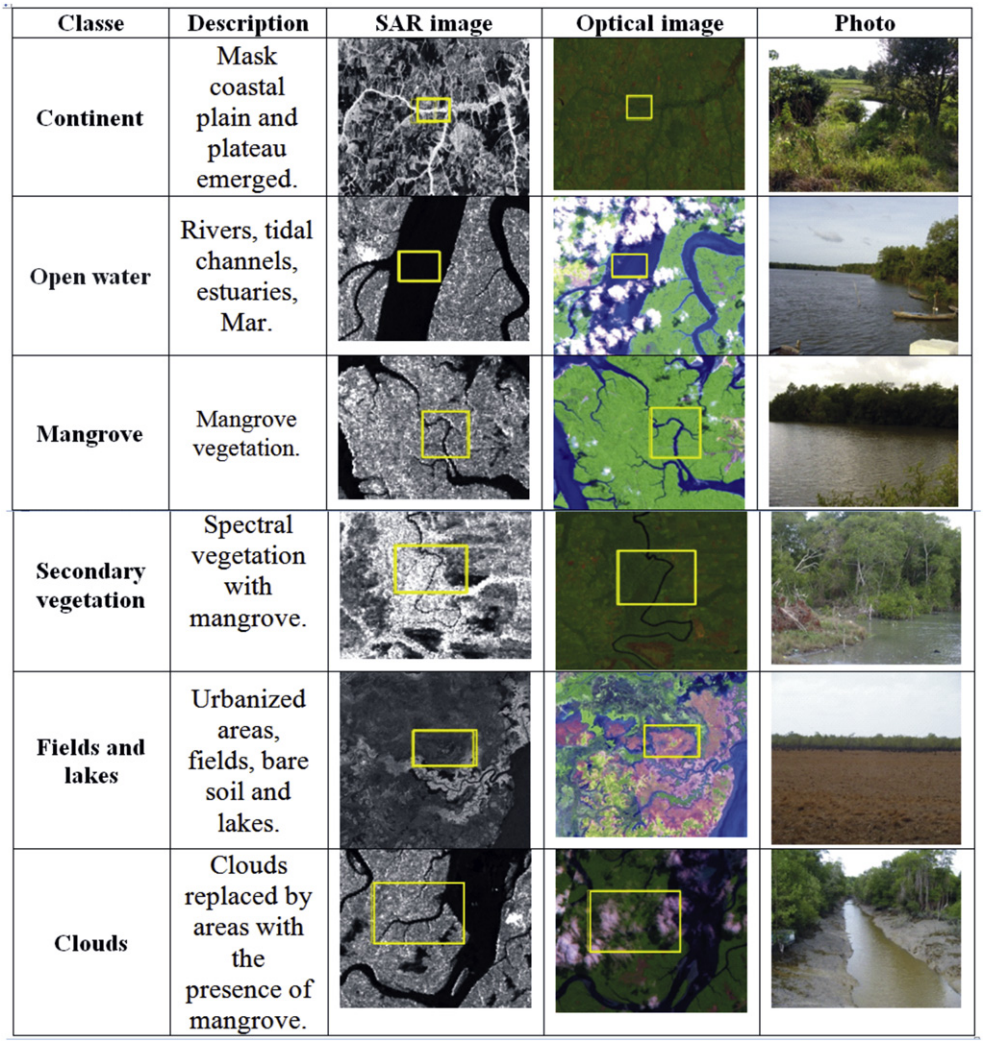

Fig. 4. Classes used in the classification of mangrove areas. The yellow rectangles indicate the position of photographs taken in the field. (For interpretation of the references to colour in this figure legend, the reader is referred to the web version of this article.)

using a combination of ground-based assessments of land covers. Digital image processing was carried out using different software suites.

The study used 18 JERS-1 SAR L-band HH-polarization scenes and 9 ALOS PALSAR Fine Beam Dual (FBD) HH and HV strips acquired in 1996 and 2008 respectively, with the JERS-1 SAR mosaic provided as part of the GRFM project. PALSAR data were provided at 50 m spatial resolution and as Level 1.1 format through the K&C Initiative. Orthorectification of these was undertaken within the Gamma SAR processing software using 90 m Shuttle Radar Topographic Mission (SRTM) data as reference. For both 1996 and 2008, 12 Landsat-5 TM images (28.8 m spatial resolution) were downloaded from the Global Land Cover Facility (GLCF), with these already radiometrically corrected and orthorectified (Tucker et al., 2004).

The characteristics of the remote sensing data are presented in Table 1. All data were provided in a geographic coordinates system using the World Geodetic System (WGS-84) as reference. The average quadratic error obtained using 1st degree polynomial corrections was less than 1 pixel. The JERS-1 SAR, ALOS PALSAR and Landsat TM mosaics are illustrated in Fig. 2.

3.2. Field data collection

In September and November 2010, field visits were made during which panoramic digital photographs and ground control points (GCPs) were acquired using global positioning receivers linked to a Global Position System (GPS). Particular focus was on identifying mangrove areas and obtaining evidence of change in extent, structure and condition. As access to the study area was limited and over 9000 km of coastline was considered, samples were only taken from a region between Belém and São Luís cities. Over the course of the field campaign, 215 GCPs were collected with 62 used to validate the classification of mangroves and 153 to validate other classes that were common in the area and which represented the interface with mangroves. During the fieldwork, sites were visited to obtain knowledge of mangrove species composition and growth stage and to document the characteristics of other land covers (Fig. 4). The GCPs were selected in areas near the shoreline and along the roads that crossed through the mangrove area as well as in areas representing the limits of mangroves and borders with other land covers. The spatial locations of the GCPs are given in Fig. 1.

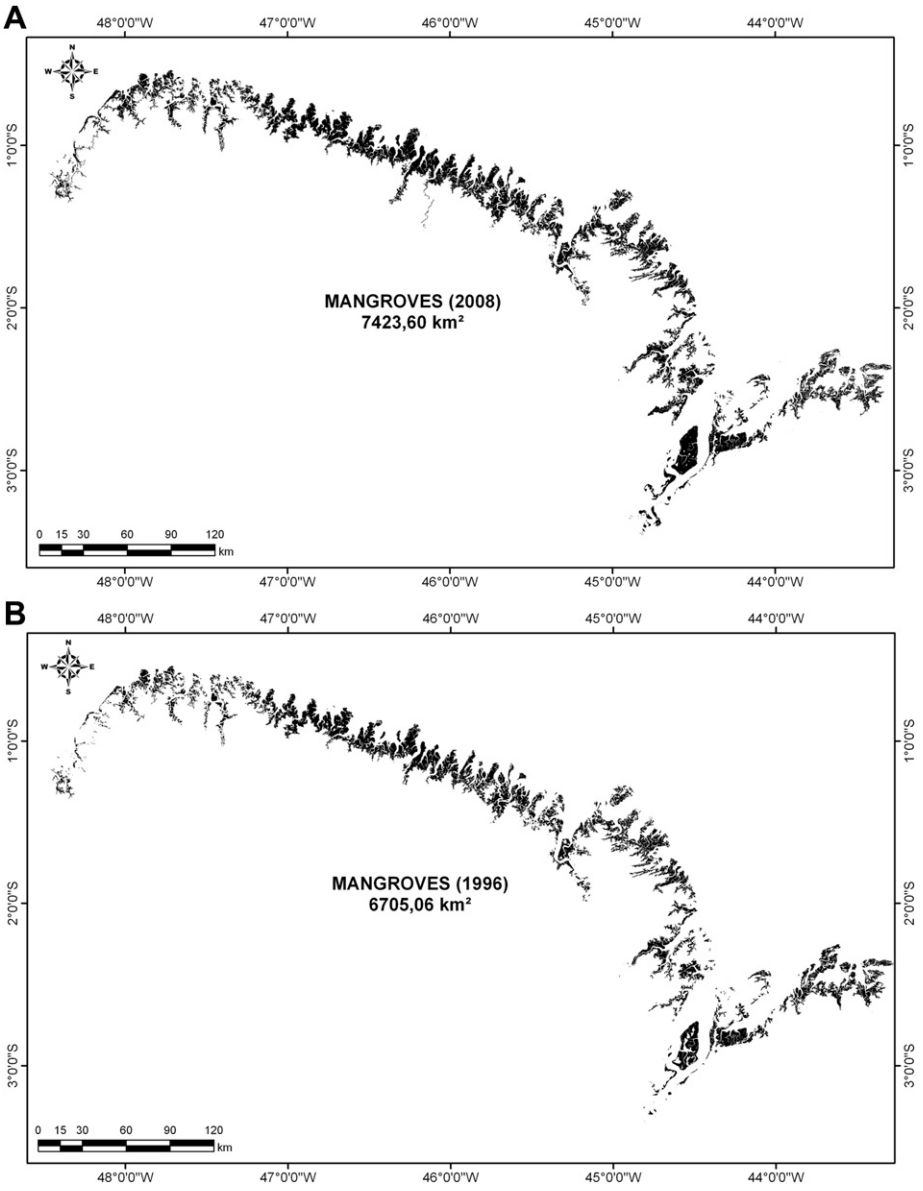

Fig. 5. Mangrove areas for 2008 (A) and 1996 (B).

3.3. Object-based segmentation and classification

Segmentation is the process of partitioning an image into groups of pixels that have similar numerical characteristics and are spatially adjacent, thereby minimizing the variability within the object (Baatz and Schäpe, 2000). Whilst many studies (e.g., Flanders et al., 2003; Wulder et al., 2009) have used a single image for segmentation, the segmentation in this study (undertaken in eCognition) used the JERS-1 SAR, ALOS PALSAR, Landsat TM and SRTM data in combination. In the segmentation, different weights were applied with the greatest attributed to the JERS-1 SAR and ALOS PALSAR (weight = 15) and as well as SRTM elevation data (weight 10). A lower weight (weight 3) was given to the Landsat TM images. Following segmentation, rules were developed to classify objects associated with mangroves, with these based on relative height (determined from the SRTM), SAR backscatter and the Landsat Thematic Mapper (TM) reflectance values. The SRTM data were first used to confine the mapping to areas below a conservative elevation value of 50 m, with this considered that the top height of most mangroves was >25 m and no more than 40 m. The SRTM provides a canopy height model (CHM) which is equivalent to a Digital Terrain Model (DTM) only in areas of low or non-vegetation. For mangroves, Simard et al. (2006) noted that the SRTM CHM, when corrected for mean sea level, was within 2 m of the height of mangroves when these were contiguous within a pixel. The height above mean sea level corresponds also to the height of the mangroves given their location on the coast, although amendments need to be made for the tidal level. To define thresholds for the classification, 79, 75 and 76 samples associated with mangroves, open water and other categories respectively (Fig. 5) were selected from within the images and used to define thresholds for subsequent classification. These samples were based primarily on interpretation of the imagery obtained through site visits in late 2010 (see later sections), during which ground-level photographs were taken.

Using the SAR data alone, the mangroves were often difficult to distinguish from proximal secondary forests and other vegetation covers and hence Landsat TM and SRTM data were also needed to define their extent. In several scenes, many mangroves were obscured by haze and hence mapping necessarily utilised the Landsat TM shortwave infrared (SWIR; band 5) reflectance values, as penetration of the atmosphere in this wavelength region was greater. Where cloud completely obscured the mangroves, SRTM data were used as these reflected height differences between the mangroves and the surrounding covers. A summary of the rules used for the classification of mangrove extent is provided in Table 2.

3.4. Object-based change detection

The segments that initially make up the mangrove class, defined using the object-based classification process in the JERS-1 1996 and ALOS PALSAR 2008 images, were exported in raster format and submitted to a segmentation process with new weights. As only one class was to be mapped, the digital numbers of 0 and 255 were assigned to represent mangroves and non-mangroves respectively. After segmentation and creation of new objects, three classes were defined with these representing the extent of mangroves in 1996 and 2008 and areas of increase, decrease and no change. The segmentation parameters utilized in the multi-resolution segmentation were the following: parameters of scale = 10, form = 0.1 and compacity = 0.5. For detecting change, the matrix files ("rasters") of the mosaics for 1996 and 2008 received weights equal to 1. After defining the classes, the objects classified were exported to ArcGIS 10.0 software in vector format. This procedure is summarized in Table 3.

3.5. Validating mangrove extent and change maps

For validation, the class of 'mangrove' was separated from other categories (i.e., water including lakes, secondary vegetation, gallery and swamp forest and non- or sparse vegetation (barren), which were merged into a single class termed "other". The error analysis was performed using the field data and observations and only for the classification undertaken in 2008, given that this year was the closest to the date of field data collection (2010). For validation of both the 2008 map and the change map, standard error matrices were constructed (Congalton, 1991; Foody, 2002) with measures of

Table 2
Classification rules (descriptors and algorithms) used to map mangrove following decision processes 1, 2, 3 and 4.

Process	Child process	Algorithm	Function / Condition (Descriptor)	Function / Condition (Descriptor)
1 - Segmentation		Multiresolution segmentation		
2 - Classification	(2.1) Classify secondary vegetation class	Assign class	10*LOG(SAR BANDA L) >= 25	CUSTOM 10LOG(SAR BANDA L)
	(2.2) Classify water class	Assign class	10*LOG(SAR BANDA L) < 25	CUSTOM 10LOG(SAR BANDA L)
	(2.3) Classify Mangrove class	Classification	[10*(mean B5 Landsat) + (mean SRTM)] 200 600	CUSTOM EQUAÇÃO 1 (200 − 600)
3 - Group	Group segments of water class	Merge region		
4 - Reclasification	(4.1) Reclassify mangrove class as secondary vegetation	Classification	Area <= 4,00,000 pixel Rel. border to Continent >= 0.12	Area Rel. border to
	(4.2) Reclassify water class as marsh and lakes	Classification	Area < 25000 pixel	Area
	(4.3) Reclassify continent as mangrove under clouds	Classification	Distance to mangrove <= 130 pixel Mean SRTM 10 21 Rel. border to mangrove <= 0.9 [10*(mean SRTM) + (mean 10*Log SAR BANDA L)] 100 250	Distance to Mean (10 − 21) Rel. border to EQUAÇÃO 2 (100 − 250)
5 - Group	Merge classes	Merge Region		

Table 3
Process trees utilized in elaborating change detection.

Process	Child process	Algorithm	Level	Function/Condition (Descriptor)
1 Segmentation	(1.1) Image segmentation	Multiresolution segmentation	1	
	(1.2) Copy of segmentation	Copy image object level	2	Copy under level 1 (1996)
	(1.3) Copy of segmentation	Copy image object level	3	Copy under level 2 (2008)
2 Classification	(2.1) Classify mangrove class 1996	Classification	2	Mean 1996 = 0
	(2.2) Classify mangrove class 2008	Classification	3	Mean 2008 = 0
3 Change detection	(3.1) Classify increased mangrove class	Classification	1	Existence of sub objects mangrove 2008 = 1 Existence of sub objects mangrove 1996 = 0
	(3.2) Classify decreased mangrove class	Classification	1	Existence of sub objects mangrove 2008 = 0 Existence of sub objects mangrove 1996 = 1
	(3.3) Classify no-change mangrove class	Classification	1	Existence of sub objects mangrove 2008 = 1 Existence of sub objects mangrove 1996 = 1

accuracy being the overall, producer's and user's (Congalton and Green, 2009) as well as the Kappa and Tau coefficients (Ma and Redmond, 1995).

4. Results

4.1. Accuracy in classification of mangrove extent and change

In 2010, 215 field sites were visited and 96% (207) were correctly classified. The Kappa and Tau coefficients of 91% and 93% indicated the improvement of the classification over a random assignment of pixels to a class (Table 4A). Of the 62 points known to be mangrove, 87% (54) were correctly classified with the remaining 13% (8) representing primary or secondary forests, marshes and open water, including lakes. A number of the 153 GCPs were collected from other areas and these were all correctly classified as a group, although some confusion with mangroves occurred, reducing in errors of omission of around 5% (i.e., a producer's accuracy of 95%). Fig. 5 presents mangroves maps for 1996 and 2008.

In the detection of change, 54 GCPs were used, with 23 and 31 representing unaltered and altered mangroves respectively, either through expansion (an increase) or retraction (decrease). Field examples of the different forms of expanding, reducing and unaltered mangroves observed when comparing the JERS-1 SAR and ALOS PALSAR are presented in Fig. 6. For areas that were unaltered, 83% were classified correctly with the remaining 17% classified as altered. Of those classified as altered, 84% (26) were correctly classified. The confusion occurred in ecotone areas, where mangrove, rainforest and gallery forest were in close proximity. In the overall classification, the overall accuracy was 83% (i.e., 45 points were correctly classified) and the Kappa and Tau coefficients were 80% and 66% respectively, which indicated a close correspondence between the classification output and the field observations (Table 4b).

Table 4
A) Error matrix in the multi-resolution and multi-sensor object-based classification oriented. B) Confusion matrix prepared to validate classification of change detection.

A)

Classification	Mangrove	Other	Total	Error of commission	User's accuracy
Mangrove	54	8	62	12.90%	87.10%
Other	0	153	153	0	100%
Total	54	161	215		
Error of omission	0%	4.96%			
Producer's accuracy	100%	95.04%			
Kappa per Class	0.9626	0.9625			
General accuracy = 96.28%		Kappa index = 0.91		Tau index = 0.93	

B)

Classification	No change	Change	Total	Error of commission	User's accuracy
No change	19	4	23	17.39%	82.60%
Change	5	26	31	16.12%	83.87%
Total	24	30	54		
Error of omission	20.83%	13.33%			
Producer's accuracy	79.16%	86.66%			
Kappa per class	0.83	0.82			
General accuracy = 83.33%		Kappa index = 0.66		Tau index = 0.67	

4.2. Status and dynamics of mangroves between 1996 and 2008

Areas of expansion and retraction of mangroves were identified between 1996 and 2008. Fig. 6 presents examples of the different forms of expansion, reduction and unaltered mangrove areas observed in the field and in SAR images.

The mangroves to the AMMC presented a growth of from 6705.05 km^2 (1996) to 7423.60 km^2 (2008). Over these 12 years, there was an increase of 1931 km^2 and a reduction of 1213 km^2 in the mangrove area, with 5493 km^2 remaining unaltered. This resulted in a net gain of 718.5 km^2 equating to 10.7% in the mangrove areas (Fig. 7). The increase in mangroves was largely observed in the upper reaches of the rivers suggesting inland salt-water intrusion. While losses were largely due to river and coastal erosion whereby large were lost, particularly towards the southwest of the study area.

5. Discussion

5.1. Object-based classifications of mangrove extent and change

Compared to pixel-based approaches which requires only spectral information-digital values (DNs) stored in the image (Singh, 1989), the use of objects to map the extent of mangrove and changes over time was beneficial for the segmentation and classification of images based on spectral and textural properties of homogenous areas, defined as objects (Baatz and Shape, 2000; Schiewe et al., 2001). Given the same image types, similar rules could also be used for classifying other objects although some manual editing was necessary. The classification was also informed by ecological knowledge of the state and dynamics of mangroves within the coastal margin.

The accuracy in the classification of mangroves was considered excellent with differences between the Kappa and Tau coefficients attributed to differences in the number of samples used for classifying the mangroves and identifying areas that were altered or otherwise. It should be noted that the points chosen for validating the classification were collected at sites where greatest confusion between classes when using SAR and optical imagery occurred. The accuracies for both extent and change mapping indicated that the object-based classification was compatible with a visual interpretation performed by an interpreter with knowledge of the terrain. This is evidenced by the close correspondence with the mangrove extension mapped by Souza-Filho (2005) from visual interpretation

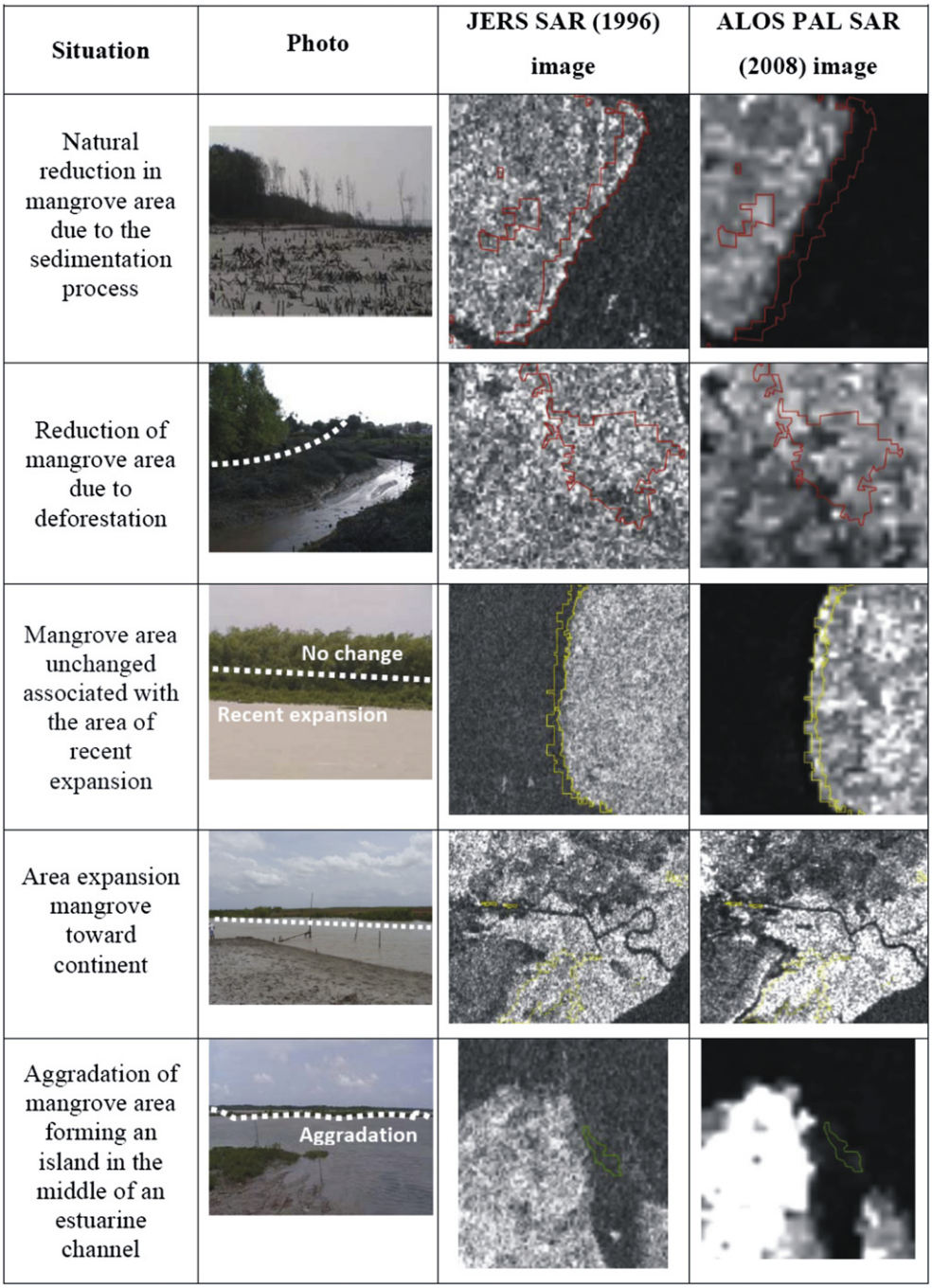

Fig. 6. Forms of expansion and reduction in the mangrove areas.

of Landsat-5 TM images, which was 7591 km^2 for the year 2000 compared to 7423.6 km^2 in 2008 (in this study).

5.2. Extent and changes in mangroves

The maps of extent confirmed that the mangroves to the east of the Amazon River mouth represent the most extensive continuous belt of mangroves globally. By comparison, the area of the mangrove forests in the Sundarbans of India and Bangladesh cover approximately 5,816 km^2 (Giri et al., 2007) whilst those of the Gulf of Papua in New Guinea, occupy an area of approximately 5,929 km^2 (Shaerman et al., 2009).

Changes in mangroves are largely the result of local human pressures in the form of deforestation and landfills for building roads and residential settlements, with this most commonly occurring where mangroves abut terrestrial land. However, the population density within the Amazon mangroves is typically low, varying from 10 to 25 inhabitants per km^2 (Souza-Filho et al., 2009). Natural losses of mangroves are associated with erosion in response to wave and tidal action, which leads to root burial by sediments coming from the inner continental shelf and death of mangroves. Despite human pressures and natural losses, an increase of 10.7% was observed with this attributed to lateral progradation and landward migration within areas of the highest elevation. These observations suggest that salinization is occurring

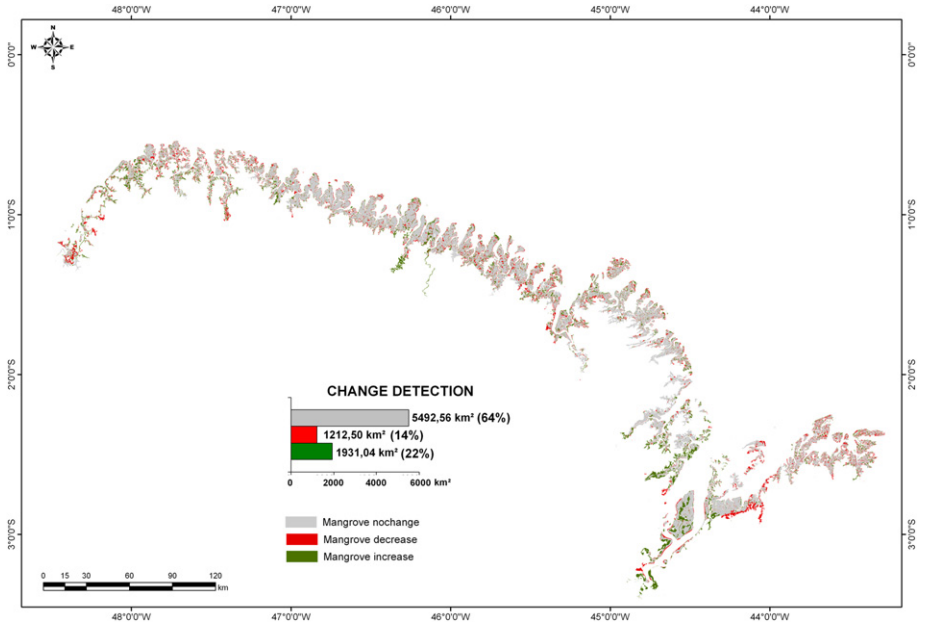

Fig. 7. Amazon mangrove forest change from 1996 to 2008.

in the upper courses of the estuaries, generating propitious areas for mangrove development with many moving upstream. Similar patterns of inland expansion have also been observed by Ellison (1993) in Bermuda and Gilman et al. (2007) in American Samoa. The process of expansion of large mangrove areas over herbaceous fresh fields on the topographically highest sectors provides evidence of relative sea level rise in the Amazon region (Cohen et al., 2009; Souza-Filho et al., 2009; Guimarães et al., 2012).

It is important to note that the process of expansion of large mangrove areas observed to the east of the Amazon River mouth is peculiar to this study area. Studies carried out in other areas with large extensions of mangroves, such as the Gulf of Papua in Papua New Guinea, show a reduction in the mangrove area for the period of 1973–2002 (Shearman, 2010), while the mangroves in the Sundarbans in Bangladesh and India remained unaltered from 1973 to 2000 (Giri et al., 2007, 2008). Furthermore, the authors cited above did not quantify variations in the mangrove areas at their boundaries inland with the mainland, which may compromise the balance in areas of mangrove expansion and reduction. In other words, the expansion and retraction analysis of mangroves were carried out only on the seaward coast and further research is needed to quantify the true changes in mangroves areas at a global level.

6. Conclusion

The combined use of optical and radar remote sensing data has been shown to benefit the mapping of mangroves and mangrove change within the AMMC, partly because of the provision of cloud-free observations by the radar but also because of different sensitivities to differences in mangroves structure and species composition. Within this framework, a multi-resolution and multi-sensor classification method highlighted promising results for discriminating mangroves areas from others types of coastal surfaces, with accuracies in the classification of extent exceeding 95% regardless of the date of acquisition and change exceeding 83%.

The mangrove forest mapped in 2008 confirms the AMMC as supporting the largest continuous mangrove area in the World, being 1500 km^2 larger than the extensive mangroves of India and Bangladesh, and one that is also increasing in extent. For the period from 1996 to 2008, an increase in the mangrove area on the order of 10% ($\sim$718 km^2) has been observed. The study has highlighted that the mapping of mangroves cannot consider these systems as static and hence regular updating is needed in order to inform on changes and the implications for conservation, economies and policy. Furthermore, an understanding of the processes of change is needed to establish the direction but also whether the causes are the consequence of natural and/or human-induced processes. For this reason, additional information on seasonal rainfall variations, river flows, tidal and sea level fluctuations and air and ocean surface temperatures are needed. Through such an approach, the contributions of climate change impacts can be better disaggregated.

The integrated approach presented in this paper showed to be efficient to quantify mangrove areas and changes in both the landward and seaward directions. The use of SAR data allowed quantifying mangrove area along the Equatorial zone, independently of season and weather conditions. These results are useful for the development of robust and reproducible remote sensing methods dedicated to the dynamic mapping of fast changing tropical coasts. Therefore, it is recommended that this method should be applied to characterize, map and monitor the global mangrove changes as planned within the Japanese Space Exploration Agency (JAXA)-ALOS Kyoto & Carbon (K&C) Initiative Global Mangrove Watch project that is set out to use ALOS and ALOS-2 data for global mangrove assessment.

Acknowledgements

The authors would like to acknowledge the financial support and field assistance provided by the Coordenação de Aperfeiçoamento de Pessoal de Nível Superior (CAPES-Brazil) and Conselho Nacional de Desenvolvimento Científico e Tecnológico (CNPq-Brazil), particularly Marine Science and Universal Announcement respectively. The authors also wish to acknowledge the technical support provided by the Threetek Solutions in Geomatica to use eCognition software and support provided by Universidade Federal do Pará – UFPA and Fundação de Amparo e Desenvolvimento da Pesquisa – FADESP. Acknowledgement is also extended to JAXA that provided JERS-1 images from GRFM Project and ALOS PALSAR images from K&C Project, and to NASA and INPE, which provided

Landsat and SRTM images. The authors are also grateful to Afonso Quaresma that leads us safely on the roads of Amazon. Finally, we would also like to thank the reviewers of this paper and their valuable contribution towards refining the manuscript.

References

Alongi, D.M., 2002. Present state and future of the world's mangrove forests. Environmental Conservation 29, 331–349.

Alongi, D.M., 2008. Mangrove forests: resilience, protection from tsunamis, and responses to global climate change. Estuarine, Coastal and Shelf Science 76, 1–13.

Baatz, M., Schape, A., 2000. Multiresolution segmentation: an optimization approach for high quality multi-scale image segmentation. In: Strbl, J., Blaschke, T. (Eds.), Angewandte Geographische Informationsverarbeitung. Wichmann, Heidelberg, pp. 12–23.

Cohen, M., Behling, H., Lara, R.J., Smith, C., Matos, H., Vedel, V., 2009. Impact of sea-level and climatic changes on the Amazon coastal wetlands during the late Holocene. Vegetation History and Archaeobotany 18, 425–439.

Congalton, R.G., 1991. A review of assessing the accuracy of classifications of remotely sensed data. Remote Sensing of Environment 49, 1671–1678.

Congalton, R.G., Green, K., 2009. Assessing the Accuracy of Remote Sensed Data: Principle and Pratices, second ed. CRC Press, Boca Raton, p. 183.

Desclée, B., Bogaert, P., Defourny, P., 2006. Forest change detection by statistical object-based method. Remote Sensing of Environment 102, 1–11.

DHN –; (DEPARTAMENTO DE HIDROGRAFIA E NAVEGAÇÃO), 2010. Tábua de Marés. Available at: http://www.mar.mil.br/dhn/chm/tabuas/index.htm (accessed 07.08.10.).

Diele, K., Araujo, A.R.R., Glaser, M., Salzmann, U., 2010. Artisanal fishery of the mangrove crab *Ucides cordatus* (Ucididae) and first steps toward a successful co-management in Bragança, North Brazil. In: Saint-Paul, U., Schneider, H. (Eds.), Mangrove Dynamics and Management in North Brazil. Springer-Verlag, Berlin, pp. 287–303.

Donato, D.C., Kauffman, J.B., Murdiyarso, D., Kurnianto, S., Stidham, M., Kanninen, M., 2011. Mangroves among the most carbon-rich forests in the tropics. Nature Geoscience 4, 293–297.

Ellison, J., 1993. Mangrove retreat with rising sea level, Bermuda. Estuarine, Coastal and Shelf Science 37, 75–87.

FAO, 2005. Global Forest Review Assessment, 2005. FAO, Rome.

Flanders, D., Hall-Beyer, M., Pereverzoff, J., 2003. Preliminary evaluation of eCognition object-based software for cut block delineation and feature extraction. Canadian Journal of Remote Sensing 29, 441–452.

Foody, G.M., 2002. Status of land cover classification accuracy assessment. Remote Sensing of Environment 80, 185–201.

Fromard, F., Veja, C., Proisy, C., 2004. Half a century of dynamic coastal change affecting mangrove shorelines of French Guiana. A case study based on remote sensing data analyses and field surveys. Marine Geology 208, 265–280.

Gilman, E., Ellison, J., Coleman, R., 2007. Assessment of mangrove response to projected relative sea-level rise and recent historical reconstruction of shoreline position. Environmental Monitoring and Assessment 124, 112–134.

Giri, C., Pengra, B., Zhu, Z., Singh, A., Tieszen, L., 2007. Monitoring mangrove forest dynamics of the sundarbans in Bangladesh and India using multi-temporal satellite data from 1973–2000. Estuarine, Coastal and Shelf Science 73, 91–100.

Giri, C., Zhu, Z., Tieszen, L.L., Singh, A., Gillette, S., Kelmelis, J.A., 2008. Mangrove forest distributions and dynamics (1975–2005) of the tsunami-affected region of Asia. Journal of Biogeography 35, 519–528.

Giri, C., Ochieng, E., Tieszen, L.L., Zhu, Z., Singh, A., Loveland, T., Masek, J., Duke, N., 2011. Status and distribution of mangrove forests of the world using earth observation satellite data. Global Ecology and Biogeography 20, 154–159.

Glaser, M., 2003. Interrelations between mangrove ecosystem, local economy and social sustainability in Caeté Estuary, North Brazil. Wetlands Ecology and Management 11, 265–272.

Green, E.P., Clark, C.D., Mumby, P.J., Edwards, A.J., Ellis, A.C., 1998. Remote sensing techniques for mangrove mapping. International Journal of Remote Sensing 19, 935–956.

Guimarães, J.T.F., Cohen, M.C.L., Pessenda, L.C.R., França, M.C., Smith, C.B., Nogueira, A.C.R., 2012. Mid- and late-Holocene sedimentary process and palaeovegetation changes near the mouth of the Amazon River. The Holocene 22, 359–370.

Herz, R., 1991. Manguezais do Brasil. Edusp, IOUSP, São Paulo, p. 227.

Kathiresan, K., Rajendran, N., 2005. Coastal mangrove forests mitigated tsunami. Estuarine, Coastal and Shelf Science 65, 601–606.

Lobo, A., 1997. Image segmentation and discriminant analysis for the identification of land cover units in ecology. IEEE Transactions on Geoscience and Remote Sensing 35, 1136–1145.

Lu, D., Mausel, P., Brondizio, E., Moran, E., 2004. Change detection techniques. International Journal of Remote Sensing 25, 2365–2407.

Lucas, R.M., Mitchell, A.L., Rosenqvist, A., Proisy, C., Melius, A., Ticehurst, C., 2007. The potential of L-band SAR for quantifying mangrove characteristics and change. Case studies from the tropics and subtropics. Aquatic Conservation: Marine & Fresh Water Ecosystems 17, 245–264.

Ma, Z., Redmond, R., 1995. Tau coefficients for accuracy assessment of classification of remote sensing data. Photogrammetric Engineering and Remote Sensing 61, 435–439, Menezes, M.P.M.d., Berger, U., Mehlig, U., 2008. Mangrove vegetation in Amazonia: a review of studies from the coast of Pará and Maranhão States, north Brazil. Acta Amazonica 38, pp. 403–420.

Menezes, M.P.M., Berger, U., Mehlig, U., 2008. Mangrove vegetation in Amazonia: a review of studies from the coast of Pará and Maranhão States, north Brazil. Acta Amazonica 38, 403–420.

Moraes, B.C., Costa, J.M.N., Costa, A.C.L., 2005. Variação espacial e temporal da precipitação no estado do Pará. Acta Amazônica 35, 207–214.

Proisy, C., Mougin, E., Fromard, F., Karam, M.A., 2000. Interpretation of polarimetric radar signatures of mangrove forests. Remote Sensing of Environment 71, 56–66.

Proisy, C., Couteron, P., Fromard, F., 2007. Predicting and mapping mangrove biomass from canopy grain analysis using Fourier-based textural ordination of IKONOS images. Remote Sensing of Environment 109, 379–392.

Prost, M.T., 1997. La mangrove de front de mer en Guyane: ses transformations sous l'influence du système de dispersion Amazonien et son suivi par télédétection. In: Kjerfve, B., Lacerda, L.D., Diop, E.H.S. (Eds.), Mangrove Ecosystem Studies in Latin America and Africa. UNESCO, Paris, pp. 111–126.

Rebelo-Mochel, F., 1997. Mangroves on São Luís Island, Maranhão Brazil. In: Kjerfve, B., Lacerda, L.D., Diop, E.H.S. (Eds.), Mangrove Ecosystem Studies in Latin America and Africa. UNESCO, Paris, pp. 145–154.

Rodrigues, S.W.P., Souza-Filho, P.W.M., 2011. Use of multi-sensor data to identify and map tropical coastal wetlands in the Amazon of Northern Brazil. Wetlands 31, 11–23.

Rosenqvist, A., Shimada, M., Chapman, B., Freeman, A., De Grandi, G.D., Saatchi, S., Rauste, Y., 2000. The global rain forest mapping project – a review. International Journal of Remote Sensing 21, 1375–1387.

Rosenqvist, A., Shimada, M., Ito, N., Watanabe, M., 2007. ALOS PALSAR: a pathfinder mission for global-scale monitoring of the environment. IEEE Transactions on Geoscience and Remote Sensing 45, 3307–3316.

Saenger, P., Hegerl, E.J., Davie, J.D.S., 1983. Global Status of Mangrove Ecosystems. Commission on Ecology. Papers N. 3. World Conservation Union (IUCN), Switzerland.

Saura, S., 2002. Effects of minimum mapping unit on land cover data spatial configuration and composition. International Journal of Remote Sensing 23, 4853–4880.

Schiewe, J., Tufte, L., Ehlers, M., 2001. Potential and problems of multi-scale segmentation methods in remote sensing. GIS. Geo-Informations-Systeme 14, 34–39.

Shearman, P.L., 2010. Recent change in the extent of mangroves in the Northern Gulf of Papua, Papua New Guinea. AMBIO 39, 181–189.

Shearman, P.L., Ash, J., Mackey, B., Bryan, J.E., Lokes, B., 2009. Forest conversion and degradation in Papua New Guinea 1972–2002. Biotropica 41, 379–390.

Simard, M., Zhang, K., Rivera-Monroy, V.H., Ross, M.S., Ruiz, P.L., Castaneda-Moya, E., Twilley, R.R., Rodriguez, E., 2006. Mapping height and biomass of mangrove forests in everglades national park with SRTM elevation data. Photogrammetric Engineering & Remote Sensing 72, 299–311.

Singh, A., 1989. Digital change detection techniques using remotely sensed data. International Journal of Remote Sensing 10, 989–1003.

Souza-Filho, P.W.M., 2005. Costa de Manguezais de Macromaré da Amazônia: cenários morfológicos, mapeamento e quantificação de áreas usando dados de sensores remotos. Revista Brasileira de Geofísica 23, 427–435.

Souza-Filho, P.W.M., Paradella, W.R., 2003. Use of synthetic aperture radar for recognition of coastal geomorphological features, land-use assessment and shoreline changes in Bragança coast, Pará, Northern Brazil. Annals of the Brazilian Academy of Sciences 75, 341–356.

Souza-Filho, P.W.M., Paradella, W.R., 2005. Use of RADARSAT-1 fine mode and Landsat-5 TM selective principal component analysis for geomorphological mapping in a macrotidal mangrove coast in the Amazon region. Canadian Journal of Remote Sensing 31, 214–224.

Souza-Filho, P.W.M., Martins, E.S.F., Costa, F.R., 2006. Using mangroves as a geological indicator of coastal changes in the Bragança macrotidal flat, Brazilian Amazon: a remote sensing data approach. Ocean &Coastal Management 49, 462–475.

Souza-Filho, P.W.M., Lessa, G.C., Cohen, M.C.L., Costa, F.R., Lara, R.J., 2009. The subsiding macrotidal barrier estuarine system of the Eastern Amazon Coast, Northern Brazil. In: Dillenburg, S.F., Hesp, P.A. (Eds.), Geology and Geomorphology of Holocene Coastal Barriers of Brazil. Springer, New York, pp. 347–375.

Souza-Filho, P.W.M., Paradella, W.R., Rodrigues, S.W.P., Costa, F.R., Mura, J.C., Gonçalves, F.D., 2011. Discrimination of coastal wetland environments in the Amazon region based on multi-polarized L-band airborne synthetic aperture radar imagery. Estuarine, Coastal and Shelf Science 95, 88–98.

Spalding, M., Kainuma, M., Collins, L., 2010. World Atlas of Mangroves, second ed. Earthscan, London, p. 336.

Tucker, C.J., Grant, D.M., Dykstra, J.D., 2004. NASA's global orthorectified Landsat data set. Photogrammetric Engineering & Remote Sensing 70, 313–322.

UNEP-WCMC, 2006. In the Front Line: Shoreline Protection and Other Ecosystem Services From Mangroves and Coral Reefs. Cambridge, UNEP-WCMC, London. p. 33.

Walter, V., 2004. Object-based classification of remote sensing data for change detection. ISPRS Journal of Photogrammetry and Remote Sensing 58, 225–238.

Wang, L., Sousa, W.P., Gong, P., Biging, G.S., 2004. Comparison of IKONOS and QuickBird images for mapping mangrove species on the Caribbean coast of Panama. Remote Sensing of Environment 91, 432–440.

Wulder, M.A., Hall, R.J., Coops, N.C., Franklin, S.E., 2009. High spatial resolution remotely sensed data for ecosystem characterization. BioScience 54, 511–521.